AN OPTIMAL METHOD TO ESTIMATE THE SPHERICAL HARMONIC COMPONENTS OF THE SURFACE AIR TEMPERATURE

SAMUEL S. SHEN
Department of Mathematical Sciences
University of Alberta
Edmonton, CANADA T6G 2G1
and
Center for Climate System Research
University of Tokyo
Tokyo 153, JAPAN

GERALD R. NORTH

AND

KWANG-Y. KIM

Climate System Research Program
Texas A&M University
College Station, TX 77843

October 4, 1995

AN OPTIMAL METHOD TO ESTIMATE THE SPHERICAL HARMONIC COMPONENTS OF THE SURFACE AIR TEMPERATURE

SUMMARY

This paper describes a method that minimizes the mean squared error (MSE) in estimating the spherical harmonic components of the surface air temperature field. The ratio of the MSE to the variance of the spherical harmonic component is expressed in terms of the length scale λ_0, and the positions and weights of the measurement stations. The weights are optimized by the condition of minimizing the sampling error. To present an analytical example, we assume the homogeneous statistics of the temperature anomaly field, and take the low frequency approximation (i.e., ignoring the time dependence). The spectra of the temperature anomaly are the coefficients of a Fourier-Legendre series of the covariance function, and they are analytically derived from a linear noise forced energy balance climate model. Consequently, the MSE, the percentage sampling error, and the signal-noise ratio are computed for a given network of stations. Our results show that: (i) the sampling errors computed from both optimal weights and uniform weights increase with respect to the order of the spherical harmonic component, and (ii) the sampling errors computed from optimal weights are significantly smaller than those from uniform weights for sufficiently dense networks. With about 60 reasonably positioned stations for sampling the spherical harmonic components T_{00}, T_{10} and T_{11}, one can get the sampling error below 10% when the optimal weights are applied. An experiment with 210 stations produces the sampling errors of less than 10% for the spherical harmonic components from T_{00} up to T_{54}.

KEY WORDS Mean square error, spherical harmonics, sampling, optimal weights, surface air temperature, noise forced EBM

1 INTRODUCTION

The field of surface air temperature anomalies is not distributed uniformly; rather, it has various spatial patterns. The global average of this field represents only one statistical description and explains only the lowest mode of climate variations (Shen *et al.*, 1994). To explain hemispherical and regional spatial variations, it is necessary to describe the features of various length scales. A systematic way to delineate these spatial patterns is to use spherical harmonics, i.e., to express the temperature anomaly field in terms of the series sum of spherical harmonic functions. The zeroth order spherical harmonic component corresponds to the global spatial average temperature while the higher order components consist of contributions from other spatial scale climate variations.

It is obvious that an accurate estimation of the higher order spherical components is essential to evaluate spatial climate variations. To appraise the accuracy of a scheme computing regional averages and variances of temperature anomalies from observational data, one has to estimate the sampling error. The purpose of this paper is to provide a method of calculating such an error when estimating various orders of spherical harmonic components from measurement data. A distinguishing feature of the paper is its use of optimal weights, which can substantially reduce the sampling error computed using uniform weights.

In order to clearly illustrate our methodology in a simple way, a few assumptions are imposed at this stage of investigation. First of all, we consider only the low temporal frequency part of the temperature anomaly field. Hence, the time variable is left out. In addition, we exclusively investigate the situation of data collected by surface stations. The sampling error of a spherical harmonic component is the accumulation of the numerical integration errors of empirical orthogonal functions of all orders weighted by the variances of the field at the corresponding modes (see our equation (18)). Obviously, a convenient way to illustrate our method mathematically is to present our scheme with an analytic

expression. This can be achieved by assuming the homogeneity of the anomaly field and a simple noise forced energy balance climate model. Then, we are able to derive analytic expressions for the sampling errors for a given network of fixed stations, or a network of a specified number of randomly positioned stations.

Once again, we have to remind our audience that the real temperature anomaly field is not homogeneous. The assumption of homogeneity is made only for the purpose of demonstrating our method more effectively, and it is not a necessary assumption for our methodology. The use of a simple climate model is also for the purpose of clear demonstration, and the massive EOF computations for the inhomogeneous statistics and the real observation data are reported in another paper.

We regard Earth as a perfect sphere of unit radius. Let the surface air temperature field be denoted by $T(\hat{\mathbf{n}})$, where $\hat{\mathbf{n}} = (\cos\phi\cos\theta, \cos\phi\sin\theta, \sin\phi)$ is the unit vector pointing from the sphere's center to the point in question, and ϕ and θ are latitude and longitude respectively. The function $T(\hat{\mathbf{n}})$ can be expanded into spherical harmonics Y_{lm}:

$$T(\hat{\mathbf{n}}) = \sum_{l=0}^{\infty} \sum_{m=-l}^{l} T_{lm} Y_{lm}(\hat{\mathbf{n}}). \tag{1}$$

The spherical harmonic components T_{lm} are determined by

$$T_{lm} = \int_{4\pi} d\Omega \; T(\hat{\mathbf{n}}) Y^*_{lm}(\hat{\mathbf{n}}), \tag{2}$$

where Y^*_{lm} is the complex conjugate of Y_{lm}. For the basics of the spherical harmonics, please refer to Arfken (1985) or other books on mathematical physics or electrodynamics.

The global average temperature is reflected in the zeroth order spherical harmonic component. The relationship between the zeroth order spherical harmonic component T_{00} and the global average $\bar{T}$ is

$$T_{00} = \frac{1}{\sqrt{4\pi}} \int_{4\pi} d\Omega \; T(\hat{\mathbf{n}}) = \sqrt{4\pi}\bar{T}, \tag{3}$$

where the global average is given by

$$\bar{T} = \frac{1}{4\pi} \int_{4\pi} d\Omega \; T(\hat{\mathbf{n}}). \tag{4}$$

The next scale involves hemispherical variation. The north and south hemispherical averages of the surface air temperature field behave quite differently. Among many different features revealed by the data from 1860 to 1990, a distinguishing one is that there was a sudden 0.3°C hemispheric average temperature increase in the northern Hemisphere in the early 1920s. But this sudden jump, perhaps considered as a discontinuity, did not appear in the southern Hemisphere (Folland *et al.*, 1992). The differences in the temperature anomaly patterns of the two hemispheres make the first order spherical component, T_{10}, non-negligible.

The sampling error due to the sparseness of stations is here assessed by the mean squared error (MSE), which is formulated in Section 2. The formula is simplified to an easy-to-use form for a given network of measurement surface stations. In Section 3, we consider the case of a given number of randomly arranged stations. Section 4 describes a simple noise forced linear energy balance climate model, with which we can calculate the spatial spectra of climate anomalies. The spectra are necessary for computing numerical values of the sampling errors at the different orders of spherical harmonic components. The method for calculating the optimal weights, which minimizes the MSE, is described in Section 5. Some numerical examples are given in Section 6. The summary and major conclusions of the paper are presented in Section 7.

2 MSE FOR SPHERICAL HARMONIC COMPONENTS

2.1 The covariance function kernel

The nature of the mean square error implies that only the first two moments of the measured field are relevant to the MSE. The temperature field under our consideration is its spatial anomaly. Hence, its first moment vanishes, i.e.

$$\langle T(\hat{\mathbf{n}}) \rangle = 0$$

where $\langle\cdot\rangle$ denotes the ensemble average. The second moment is described by its covariance function, which can be regarded as a symmetric kernel of an integral operator:

$$K(\hat{\mathbf{n}}, \hat{\mathbf{n}}') = \langle T(\hat{\mathbf{n}}) T(\hat{\mathbf{n}}') \rangle. \tag{5}$$

All its eigenvalues are real. The symmetric expansion (or called the Karhunen-Loève expansion) of this kernel is

$$\langle T(\hat{\mathbf{n}}) T(\hat{\mathbf{n}}') \rangle = \sum_{n=1}^{\infty} \lambda_n \psi_n(\hat{\mathbf{n}}) \psi_n(\hat{\mathbf{n}}'). \tag{6}$$

Here, $(\lambda_n, \psi_n(\hat{\mathbf{n}}))$ are the eigenpairs of the integral operator K:

$$\int_{4\pi} d\Omega \;\; K(\hat{\mathbf{n}}, \hat{\mathbf{n}}') \psi_n(\hat{\mathbf{n}}') = \lambda_n \psi_n(\hat{\mathbf{n}}), \quad n = 1, 2, 3, \cdots. \tag{7}$$

If all the eigenvalues are different, the different eigenfunctions are orthogonal:

$$\int_{4\pi} d\Omega \;\; \psi_m(\hat{\mathbf{n}}) \psi_n(\hat{\mathbf{n}}') = \delta_{mn} \tag{8}$$

where δ_{mn} is the Kronecker delta. There are some cases where one eigenvalue corresponds to several eigenfunctions. In these cases, one can still orthogonalize the eigenfunctions in this eigenspace so that different eigenfunctions are still orthogonal. A homogeneous field is such a case. By definition, when we say that a field is homogeneous, we mean that

$$K(\hat{\mathbf{n}}, \hat{\mathbf{n}}') = K(|\hat{\mathbf{n}} - \hat{\mathbf{n}}'|),$$

or

$$\langle T(\hat{\mathbf{n}}) T(\hat{\mathbf{n}}') \rangle = \sigma^2 \; \rho(\hat{\mathbf{n}} \cdot \hat{\mathbf{n}}') = \sigma^2 \rho(x) \tag{9}$$

where $\sigma^2 = \langle T^2(\hat{\mathbf{n}}) \rangle$ is the low frequency point-variance of the temperature field at point $\hat{\mathbf{n}}$. Note the $x = (\hat{\mathbf{n}} \cdot \hat{\mathbf{n}}')$ is the cosine of the opening angle between the directions (stations) $\hat{\mathbf{n}}$ and $\hat{\mathbf{n}}'$. The correlation function $\rho(x)$ is dimensionless and normalized by $\rho(x = 1) = 1$.

An important consequence of the homogeneity assumption is that the spectra of the covariance field consist only of the coefficients of the Fourier-Legendre series of the function $\rho(x)$:

$$\rho_n = \frac{1}{2} \int_{-1}^{1} dx \; \rho(x) P_n(x), \quad (n = 0, 1, 2, 3, \cdots). \tag{10}$$

Correspondingly, the correlation function $\rho(x)$ is expressed in a series sum of Legendre polynomials:

$$\rho(x) = \sum_{n=0}^{\infty} (2n+1)\, \rho_n\, P_n(x). \tag{11}$$

Now we apply the addition theorem for Legendre polynomials:

$$P_n(\hat{\mathbf{n}} \cdot \hat{\mathbf{n}}') = \frac{4\pi}{2n+1} \sum_{k=-n}^{n} Y_{nk}(\hat{\mathbf{n}}) Y_{nk}^*(\hat{\mathbf{n}}') \quad \text{(Addition theorem)}. \tag{12}$$

The covariance function of a homogeneous field can now be written as

$$\langle T(\hat{\mathbf{n}}) T(\hat{\mathbf{n}}') \rangle = \sum_{n=0}^{\infty} \sum_{k=-n}^{n} 4\pi\sigma^2 \rho_n\, Y_{nk}(\hat{\mathbf{n}}) Y_{nk}^*(\hat{\mathbf{n}}'). \tag{13}$$

Hence, the spherical harmonics $Y_{nk}(\hat{\mathbf{n}})$ are now the eigenfunctions (EOFs), and one eigenvalue $4\pi\sigma^2\rho_n$ corresponds to $2n+1$ different eigenfunctions $Y_{nk}(\hat{\mathbf{n}})$, $(k = -n, \cdots, n-1, n)$. By the orthogonality theorem of spherical harmonics

$$\int_{4\pi} d\Omega\; Y_{lm}(\hat{\mathbf{n}}) Y_{nk}^*(\hat{\mathbf{n}}) = \delta_{ln}\delta_{mk} \quad \text{(Orthogonality property)}, \tag{14}$$

we know that each pair of eigenfunctions are orthogonal.

2.2 The MSE formula

We use the data from N stations at points $\hat{\mathbf{n}}_1$, $\hat{\mathbf{n}}_2$, $\cdots$, $\hat{\mathbf{n}}_N$ to estimate the spherical harmonic component T_{lm} defined by (2). The linear estimator is

$$\hat{T}_{lm} = \sum_{j=1}^{N} w_j^{(lm)} T(\hat{\mathbf{n}}_j) Y_{lm}^*(\hat{\mathbf{n}}_j). \tag{15}$$

This is the Riemann sum of the integral (2). The surface of the unit sphere is partitioned into N sub-regions and the weight $w_j^{(lm)}$ is the area of the jth sub-region $(j = 1, 2, \cdots, N)$. Hence the weights $w_j^{(lm)}$ $(j = 1, 2, \cdots, N)$ are real-valued and satisfy the normalization condition

$$\sum_{j=1}^{N} w_j^{(lm)} = 4\pi. \tag{16}$$

The MSE for estimating T_{lm} is defined as

$$\epsilon^2_{(lm)} = \langle |T_{lm} - \hat{T}_{lm}|^2 \rangle. \tag{17}$$

This can be re-written into:

$$\begin{aligned}
\epsilon^2_{(lm)} &= \left\langle \left| \int_{4\pi} d\Omega \;\; T(\hat{\mathbf{n}}) \left[1 - w^{(lm)}(\hat{\mathbf{n}})\right] Y^*(\hat{\mathbf{n}}) \right|^2 \right\rangle \\
&= \int_{4\pi} d\Omega \int_{4\pi} d\Omega' \;\; \langle T(\hat{\mathbf{n}}) T(\hat{\mathbf{n}}') \rangle \left[1 - w^{(lm)}(\hat{\mathbf{n}})\right] \left[1 - w^{(lm)}(\hat{\mathbf{n}}')\right] Y^*_{lm}(\hat{\mathbf{n}}) Y_{lm}(\hat{\mathbf{n}}') \\
&= \sum_{n=1}^{\infty} \lambda_n |\psi_{n,lm} - \hat{\psi}_{n,lm}|^2
\end{aligned} \tag{18}$$

where

$$w^{(lm)}(\hat{\mathbf{n}}) = \sum_{j=1}^{N} w_j^{(lm)} \delta(\hat{\mathbf{n}} - \hat{\mathbf{n}}_j), \tag{19}$$

$$\psi_{n,lm} = \int_{4\pi} d\Omega \;\; \psi_n(\hat{\mathbf{n}}) Y^*_{lm}(\hat{\mathbf{n}}), \tag{20}$$

and

$$\hat{\psi}_{n,lm} = \sum_{j=1}^{N} w_j^{(lm)} \psi_n(\hat{\mathbf{n}}_j) Y^*_{lm}(\hat{\mathbf{n}}_j). \tag{21}$$

This last formula is a numerical integration of $\psi_{n,lm}$. Because

$$\lambda_n = \langle | \int_{4\pi} d\Omega \;\; T(\hat{\mathbf{n}}) \psi_n(\hat{\mathbf{n}}) |^2 \rangle, \tag{22}$$

one can see that the sampling error given by equation (18) is the accumulation of the numerical integration errors of all orders of EOFs weighted by the variances of the corresponding modes. This clear physical meaning is quite interesting.

If the field is homogeneous, then the spherical harmonics are the EOFs as pointed out in the above sub-section:

$$\lambda_n \leftrightarrow 4\pi\sigma^2\rho_n, \qquad \psi_n(\hat{\mathbf{n}}) \leftrightarrow Y_{nk}(\hat{\mathbf{n}}), \quad k = -n, \cdots, n-1, n.$$

Then the MSE formula (18) becomes

$$\epsilon^2_{(lm)} = \sum_{n=0}^{\infty} \sum_{k=n}^{n} 4\pi\sigma^2\rho_n |\delta_{nl}\delta_{km} - \sum_{j=1}^{N} w_j^{(lm)} Y_{nk}(\hat{\mathbf{n}}_j) Y^*_{lm}(\hat{\mathbf{n}}_j)|^2. \tag{23}$$

Using the addition theorem again, one can reduce the MSE formula (23) to an easy-to-compute form:

$$\frac{\epsilon^2_{(lm)}}{4\pi\sigma^2} = \sum_{n=0}^{\infty}(2n+1)\rho_n\frac{1}{4\pi}\sum_{i,j=1}^{N} w_i^{(lm)}w_j^{(lm)}P_n(\hat{\mathbf{n}}_i\cdot\hat{\mathbf{n}}_j)Y^*_{lm}(\hat{\mathbf{n}}_i)Y_{lm}(\hat{\mathbf{n}}_j) + \rho_l\left(1-2\sum_{j=1}^{N}w_j^{(lm)}|Y_{lm}(\hat{\mathbf{n}}_j)|^2\right). \quad (24)$$

Thus, the sampling error is explicitly expressed in terms of a series sum of spectral components whose coefficients are functions of the positions and weights of the stations. And the spectra ρ_n $(n = 0, 1, 2, \cdots)$ can be obtained from a homogeneous climate model. For the simple noise forced energy balance model, the detailed calculations of the spectra are given in Section 4.

In the rest of this section, in order to quickly render certain sampling properties, we set the weights to be uniform: $w_j^{(lm)} = 4\pi/N$. The uniform weights, which yield an arithmetic average, in general are not the optimal ones. But if the correlation between the data from each pair of stations is small, it can be easily shown that the uniform weights are optimal. So when using a sparse network of stations to measure the spherical harmonic components T_{lm}, the uniform weights may be approximately the optimal ones. The computation for optimal weights in general cases is explained in Section 5.

Now, let us consider some special cases. The first case is the global average long time mean of the temperature field. This case estimates the zeroth order $(m = l = 0)$ spherical harmonic coefficient for the temperature anomaly. The formula (24) is reduced to

$$\frac{\epsilon^2_{(00)}}{4\pi\sigma^2} = \sum_{n=1}^{\infty}(2n+1)\rho_n\frac{1}{N^2}\sum_{i,j=1}^{N}P_n(\hat{\mathbf{n}}_i\cdot\hat{\mathbf{n}}_j). \quad (25)$$

This expression was obtained earlier by North *et al.* (1992).

The second example is the estimation of T_{10}. Note that

$$Y_{10}(\hat{\mathbf{n}}) = \sqrt{\frac{3}{4\pi}}\sin\phi, \quad (26)$$

where ϕ is the latitude. Hence $T_{10}(\hat{\mathbf{n}})$ represents the weighted zonally average of $T(\hat{\mathbf{n}})$ and signifies the asymmetry of the largest scales between the two hemispheres. The MSE

formula (24) is now reduced to

$$\frac{\epsilon^2_{(10)}}{4\pi\sigma^2} = \sum_{n=0}^{\infty}(2n+1)\rho_n \frac{3}{N^2}\sum_{i,j=1}^{N} P_n(\hat{\mathbf{n}}_i \cdot \hat{\mathbf{n}}_j)\sin\phi_i \sin\phi_j + \rho_1\left(1 - \frac{6}{N}\sum_{j=1}^{N}\sin^2\phi_j\right). \tag{27}$$

If the network is chosen in such a way that

$$\sum_{i=1}^{N}\sin\phi_i = 0, \tag{28}$$

then the zeroth order spectrum ρ_0 has no contribution to the sampling error.

The third example is $N = 1$. Because of the homogeneity assumption, the MSE is independent of the location of the station. Let us put this station on the North Pole. Using the following formulas

$$P_n(1) = 1, \tag{29}$$

and

$$Y^2_{lm}(\hat{\mathbf{n}} = (0,0,1)) = \frac{2l+1}{4\pi}\delta_{m0}, \tag{30}$$

one can reduce the MSE formula (24) to

$$\frac{\epsilon^2_{(lm)}}{4\pi\sigma^2} = (2l+1)\delta_{m0}\sum_{n=0}^{\infty}(2n+1)\rho_n + (1 - 2(2l+1)\delta_{m0})\,\rho_l. \tag{31}$$

If we consider using one station to measure the global average temperature anomalies, the sampling error is

$$\frac{\epsilon^2_{(00)}}{4\pi\sigma^2} = \sum_{n=1}^{\infty}(2n+1)\rho_n. \tag{32}$$

Further, by formula (11) we have

$$\rho(1) = \sum_{n=0}^{\infty}(2n+1)\rho_n = 1, \tag{33}$$

and the expression (32) can be reduced to that given by North *et al.* (1992):

$$\frac{\epsilon^2_{(00)}}{4\pi\sigma^2} = 1 - \rho_0. \tag{34}$$

It indicates that the sampling error is inversely proportional to the variance explained by the zeroth order spectrum.

For the T_{10} component of the anomaly field, the sampling error is

$$\frac{\epsilon^2_{(10)}}{4\pi\sigma^2} = 3\rho_0 + 4\rho_1 + 3\sum_{n=2}^{\infty}(2n+1)\rho_n. \tag{35}$$

In general, $\rho_0 \geq 0$ and $\rho_1 \geq 0$, which imply that

$$\epsilon^2_{(10)} > (4/3)\epsilon^2_{(00)}. \tag{36}$$

Similarly, one can show that

$$\epsilon^2_{(20)} > 3.2\epsilon^2_{(00)}. \tag{37}$$

These simple comparisons are the manifestation of the fact that in order to achieve the same accuracy of measurement more stations are required for higher order spherical harmonic components than for lower order components as one would expect intuitively. Numerical examples in Section 6 further support this conclusion.

3 RANDOM DISTRIBUTION OF THE STATIONS

Historically, the positions of the measurement stations were not planned globally. Instead, they were irregularly distributed over the earth surface, mostly on land. Let us consider the case that stations are randomly distributed. The simplest possible case is the independent uniform distribution of the stations. Namely, the probability distribution function $\wp(\hat{\mathbf{n}}_1, \hat{\mathbf{n}}_2, \cdots, \hat{\mathbf{n}}_N)$ has the following properties:

$$\wp(\hat{\mathbf{n}}_1, \hat{\mathbf{n}}_2, \cdots, \hat{\mathbf{n}}_N) = \wp(\hat{\mathbf{n}}_1)\wp(\hat{\mathbf{n}}_2)\cdots\wp(\hat{\mathbf{n}}_N) \quad \text{(Independence)}, \tag{38}$$

$$\wp(\hat{\mathbf{n}}_j) = \frac{1}{4\pi} \quad (j = 1, 2, \cdots, N) \quad \text{(Uniform distribution)}. \tag{39}$$

Since $\hat{\mathbf{n}}_1$, $\hat{\mathbf{n}}_2$, $\cdots$, $\hat{\mathbf{n}}_N$ are random variables, the MSE $\epsilon^2_{(lm)}(\hat{\mathbf{n}}_1, \hat{\mathbf{n}}_2, \cdots, \hat{\mathbf{n}}_N)$ given by the formula for fixed station positions is a function of these variables. We are now interested

in the expectation value $E^2_{(lm)}$ of $\epsilon^2_{(lm)}(\hat{\mathbf{n}}_1, \hat{\mathbf{n}}_2, \cdots, \hat{\mathbf{n}}_N)$:

$$E^2_{(lm)} = \int d\Omega_1 \int d\Omega_2 \cdots \int d\Omega_N \, \epsilon^2_{(lm)}(\hat{\mathbf{n}}_1, \hat{\mathbf{n}}_2, \cdots, \hat{\mathbf{n}}_N) \wp(\hat{\mathbf{n}}_1, \hat{\mathbf{n}}_2, \cdots, \hat{\mathbf{n}}_N). \tag{40}$$

¿From (24) with uniform weighting, after some algebraic manipulations, one can obtain

$$\frac{E^2_{(lm)}}{4\pi\sigma^2} = \frac{1-\rho_l}{N} \tag{41}$$

It is well known that when sampling a spatially white noise field, the mean squared sampling error is $1/N$. Thus, the above formula explicitly shows how much the correlation spectrum can contribute to reduce the error of sampling white noise. A similar expression was obtained earlier for $l = 0$ by North *et al.* (1992) and Hardin *et al.* (1992). Comparing this expression with formula (32), we have

$$(E^{[N]}_{(00)})^2 = \frac{1}{N}(\epsilon^{[1]}_{(00)})^2. \tag{42}$$

The superscript $[N]$ signifies the number of the stations. If $N = 1$, then the sampling error is independent of the location of the station. This is one of the consequences of the homogeneity assumption of the anomaly field. In addition, it manifests the fact that the sampling error incurred in using N stations is equivalent to that in using one station that measures N times independently, say one station for each of N independent planets. But for the real climatology problem, we know that the sampling error from N independent measurements is smaller than that from N simultaneous measurements when N is larger than a certain number, which is about 25, because there is a redundancy in the network of stations that perform simultaneous measurements. This is due to the positive correlations among the neighborhood stations since the correlation length for annual mean temperature field is about 2000 [km] (Hansen and Lebedeff, 1987; Kim and North, 1991, 1993).

4 SPECTRA DERIVED FROM NOISE FORCED EBM

In the above two sections, MSE formulas for both N fixed stations and N randomly and uniformly distributed stations are obtained. Yet, in order to get numerical output, one

has to know the values of ρ_n, which can be found by using either a climate model or real data. Here we consider the case of a simple climate model which is a white noise forced linear energy balance model given by

$$\tau_0 \frac{\partial}{\partial t} T(\hat{\mathbf{n}}, t) - \lambda_0^2 \nabla^2 T(\hat{\mathbf{n}}, t) + T(\hat{\mathbf{n}}, t) = F(\hat{\mathbf{n}}, t) \tag{43}$$

where $T(\hat{\mathbf{n}}, t)$ is the local departure of the temperature from its climatology; τ_0 is an inherent time scale and λ_0 is an inherent length scale. As mentioned in the introduction, we are interested only in the low frequency limit of the climate process in this paper. With this limit the time dependent term in the above model drops out. Hence we simply consider the time independent model. The unit of the length scale λ_0 is the Earth radius. The forcing function is a spatial white noise, i.e.,

$$\langle F(\hat{\mathbf{n}}) F(\hat{\mathbf{n}}') \rangle = \sigma_F^2 \delta(\hat{\mathbf{n}} - \hat{\mathbf{n}}'), \tag{44}$$

where δ is the Dirac delta function. The time independent noise forced EBM (energy balance model) is

$$-\lambda_0^2 \nabla^2 T(\hat{\mathbf{n}}) + T(\hat{\mathbf{n}}) = F(\hat{\mathbf{n}})\,. \tag{45}$$

The spherical harmonic expansions for $T(\hat{\mathbf{n}})$ and $F(\hat{\mathbf{n}})$ are

$$T(\hat{\mathbf{n}}) = \sum_{l=0}^{\infty} \sum_{m=-l}^{l} T_{lm} Y_{lm}(\hat{\mathbf{n}}), \tag{46}$$

$$F(\hat{\mathbf{n}}) = \sum_{l=0}^{\infty} \sum_{m=-l}^{l} F_{lm} Y_{lm}(\hat{\mathbf{n}}). \tag{47}$$

Substituting these two expressions into the model equation (45), we can obtain

$$T_{lm} = \frac{F_{lm}}{1 + \lambda_0^2 l(l+1)}. \tag{48}$$

Substituting (46) into the left hand of (9) and using the Fourier-Legendre expansion (11) and the addition theorem for the spherical harmonic functions (12), we have

$$\sum_{l=0}^{\infty} \sum_{m=-l}^{l} \sum_{l'=0}^{\infty} \sum_{m'=-l'}^{l'} \langle T_{lm} T_{l'm'}^* \rangle Y_{lm}(\hat{\mathbf{n}}) Y_{l'm'}^*(\hat{\mathbf{n}}') = \sigma^2 \sum_{n=0}^{\infty} \rho_n 4\pi \sum_{k=-n}^{n} Y_{nk}(\hat{\mathbf{n}}) Y_{nk}^*(\hat{\mathbf{n}}'). \tag{49}$$

This equality and equation (48) imply that

$$\rho_n = \frac{\langle |F_{nm}|^2 \rangle / (4\pi\sigma^2)}{[1+\lambda_0^2 n(n+1)]^2}, \quad n = 0, 1, 2, \cdots. \tag{50}$$

Here $\langle |F_{nm}|^2 \rangle$ can be found from the white noise assumption (44) and the expansion (47):

$$\sum_{l=0}^{\infty} \sum_{m=-l}^{l} \sum_{l'=0}^{\infty} \sum_{m'=-l'}^{l'} \langle F_{lm} F^*_{l'm'} \rangle Y_{lm}(\hat{\mathbf{n}}) Y^*_{l'm'}(\hat{\mathbf{n}}') = \sigma_F^2 \sum_{n=0}^{\infty} \sum_{k=-n}^{n} Y_{nk}(\hat{\mathbf{n}}) Y^*_{nk}(\hat{\mathbf{n}}'). \tag{51}$$

This implies that

$$\langle F_{lm} F^*_{l'm'} \rangle = \sigma_F^2 \delta_{ll'} \delta_{mm'}. \tag{52}$$

When $n = 0$ in (50), we have

$$\rho_0 = \frac{\sigma_F^2}{4\pi\sigma^2}. \tag{53}$$

This ρ_0 can be determined by the normalization condition $\rho(x = 1) = 1$, i.e.,

$$\sum_{n=0}^{\infty} (2n+1) \frac{\rho_0}{[1+\lambda_0^2 n(n+1)]^2} P_n(1) = 1. \tag{54}$$

Noting that $P_n(1) = 1$ $(n = 0, 1, 2, \cdots)$, we have

$$\rho_0 = \frac{1}{\sum_{n=0}^{\infty} (2n+1)/[1+\lambda_0^2 n(n+1)]^2}. \tag{55}$$

Hence ρ_0 is only a function of the length scale λ_0. The larger the λ_0 is, the more variance is explained by the spectral component ρ_0. Figure 1 shows the relationship between ρ_0 and λ_0, which, of course, is a monotonically increasing function. The value of λ_0 is determined by the length scale of the anomaly field. For the annual mean field, EBM length scale is about 2000 km (Kim and North, 1991). If we take the radius of the earth to be 6367 km, λ_0 takes the value: $2000/6367 = 0.3141$. The corresponding ρ_0 is 0.0954. Thus, the zeroth order spectral component ρ_0 explains about 10% of the low frequency point variance of the surface air temperature.

To evaluate the effectiveness of a network, it is common to use either the signal-noise ratio or the percentage sampling error. They are defined respectively by:

$$\Lambda^{[N]}_{(lm)} = \frac{\langle |T_{lm}|^2 \rangle}{\langle |\hat{T}_{lm} - T_{lm}|^2 \rangle} = \frac{\sigma^2_{(lm)}}{\epsilon^2_{(lm)}}, \tag{56}$$

$$V_{(lm)}^{[N]} = \frac{\epsilon_{(lm)}^2}{\epsilon_{(lm)}^2 + \sigma_{(lm)}^2} \times 100\% = \frac{1}{1 + \Lambda_{(lm)}^{[N]}} \times 100\%. \tag{57}$$

The signal-noise ratio and the percentage sampling error for the randomly distributed stations are defined in the similar way:

$$R\Lambda_{(lm)}^{[N]} = \frac{\sigma_{(lm)}^2}{E_{(lm)}^2}, \tag{58}$$

$$RV_{(lm)}^{[N]} = \frac{E_{(lm)}^2}{E_{(lm)}^2 + \sigma_{(lm)}^2} \times 100\%. \tag{59}$$

By (41), we have

$$R\Lambda_{(lm)}^{[N]} = \frac{N\rho_l}{1 - \rho_l}, \tag{60}$$

$$RV_{(lm)}^{[N]} = \frac{1 - \rho_l}{1 + (N-1)\rho_l} \times 100\%. \tag{61}$$

These results are further depicted in Figures 2 and 3, in which the spectra ρ_l are determined by (50). Figure 2 shows that for the zeroth order spherical harmonic component the percentage sampling error is less than 10% when $N > 100$. The sampling error quickly rises as the spherical harmonic mode number l increases. From our experience of generating random numbers in an interval, we have found that many realizations can result in the points distributed in a highly nonuniform manner. Hence in practice, the arranged networks tend to have better uniformity than the average of the uniform random distributions. Thus, the sampling error for a given network of N stations tends to be smaller than the ensemble average $E_{(lm)}^2$, which, in principle, should agree with the result of Monte Carlo simulations. In this sense, one may regard $E_{(lm)}^2$ as an upper bound of the sampling error by N reasonably and uniformly positioned stations.

For climatological reference, we would like to compare the MSE resulting from sampling T_{lm} with the variance of the same component, which is

$$\sigma_{(lm)}^2 = \left\langle |T_{lm}|^2 \right\rangle \tag{62}$$

Using the covariance relation (9) and formula (50), one can derive that

$$\sigma_{(lm)}^2 = 4\pi\sigma^2\rho_l \ . \tag{63}$$

This m-independence property of $\sigma^2_{(lm)}$ is the consequence of the assumptions: (i) white noise forcing which has neither l nor m preference, and (ii) the linear homogeneous energy balance model which has no m preference either and transforms the forcing to response linearly and conformally.

With the above and the formula for ρ_l, the MSE formulas (24) and (41) can be written as:

$$\frac{\epsilon^2_{(lm)}}{\sigma^2_{(lm)}} = \sum_{n=0}^{\infty} \frac{[1+\lambda_0^2 l(l+1)]^2(2n+1)}{[1+\lambda_0^2 n(n+1)]^2} \frac{1}{4\pi} \sum_{i,j=1}^{N} w_i^{(lm)} w_j^{(lm)} P_n(\hat{\mathbf{n}}_i \cdot \hat{\mathbf{n}}_j) Y^*_{lm}(\hat{\mathbf{n}}_i) Y_{lm}(\hat{\mathbf{n}}_j)$$
$$+ \ 1 - 2\sum_{j=1}^{N} w_j^{(lm)} |Y_{lm}(\hat{\mathbf{n}}_j)|^2 \ , \tag{64}$$

$$\frac{E^2_{(lm)}}{\sigma^2_{(lm)}} = \frac{[1+\lambda_0^2 l(l+1)]^2 - \rho_0}{N\rho_0}. \tag{65}$$

These formulas will be used to get numerical results.

5 COMPUTATION OF OPTIMAL WEIGHTS

In the discussion of Section 2, we took all the weights to be equal. Obviously, we do not have to choose the weights in this way. For a given network of stations, it is clear that the best result is to choose the values of the weights in such a way that the sampling error becomes minimum. These weights are called the optimal weights. Therefore, we are going to minimize $\epsilon^2_{(lm)}$ determined by (64) under the normalization condition (16). The Lagarange function is

$$J[w_1^{(lm)}, w_2^{(lm)}, \cdots, w_N^{(lm)}] = \epsilon^2_{(lm)}/\sigma^2_{(lm)} + 2\Lambda(4\pi - \sum_{i=1}^{N} w_i^{(lm)}), \tag{66}$$

where Λ is the Lagarange multiplier. Then the conditions for critical point

$$\frac{\partial J}{\partial w_j^{(lm)}} = 0, \quad (j = 1, 2, \cdots, N) \tag{67}$$

and the normalization condition (16) result in the following linear equations:

$$\sum_{i=1}^{N} w_i^{(lm)} \left[\sum_{n=0}^{\infty} (2n+1)\rho_n P_n(\hat{\mathbf{n}}_i \cdot \hat{\mathbf{n}}_j)\right] \Re\left(Y^*_{lm}(\hat{\mathbf{n}}_i) Y_{lm}(\hat{\mathbf{n}}_j)\right) - \Lambda$$

$$= 4\pi\rho_l |Y_{lm}(\hat{\mathbf{n}}_j)|^2, \qquad (j = 1, 2, \cdots, N), \tag{68}$$

$$\sum_{i=1}^{N} w_i^{(lm)} = 4\pi. \tag{69}$$

Here the spectra ρ_n are determined by (50) in Section 4. Hence, for a given network of stations, one can solve the above $N+1$ linear equations to find the optimal weights $w_1^{(lm)}$, $w_2^{(lm)}$, $\cdots$, $w_N^{(lm)}$, and Λ. With these optimal weights, one can use formula (64) to find the minimal sampling error.

If all the stations are independent, we have

$$\sum_{n=0}^{\infty} (2n+1)\rho_n P_n(\hat{\mathbf{n}}_i \cdot \hat{\mathbf{n}}_j) = \rho(\hat{\mathbf{n}}_i \cdot \hat{\mathbf{n}}_j) = \delta_{ij}. \tag{70}$$

This results in the uniform weights $w_i^{(lm)} = 4\pi/N$, $i = 1, 2, \cdots, N$, as the unique solution to the equations (68) and (69). Therefore, if there is a non-zero cross correlation between a pair of stations, the optimal weights are definitely not uniform.

Of course, we expect the sampling error to be smaller when the optimal weights are applied. Numerical examples in the next section show that the optimal weights can significantly reduce the sampling errors.

6 Numerical examples

With the development of physical intuition and mathematical formulation, we proceed to networks of many stations. It appears that it is impossible to find an analytic expression for the sum of the infinite series (64), when there are many stations, even for uniform weighting. Therefore, we carried out numerical computations. The numerical results for both the optimal weights and the uniform weights are included in Table 1. In this numerical test, we considered four different networks.

Net I consists of four rings of six stations at latitudes: 50°S, 15°S, 15°N, and 50°N and longitudes: 150°W, 90°W, 30°W, 30°E, 90°E, and 150°E. Net II consists of eight rings of eight stations and it equally partitions the latitude-longitude map. The stations

in the first column are on the 157.5°W longitude line. Net III has 62 stations. It is the commonly referred Angell-Korshover network determined by WMO in 1958 (Trenberth and Olson, 1992), with the station on the south pole excluded. Net IV is a $24^\circ \times 12^\circ$ network. The stations in the first column are on the 168°W longitude line. This dense network is designed to estimate the higher order spherical harmonic components. It even samples T_{54} with less than 10% error when the optimal weights are applied.

Table 1 includes the results of the percentage sampling errors and the signal-noise ratios of the first 10 modes for the above four networks. In order to expose the advantage of the optimal weighting scheme, we list the uniform weighting results in parenthesis for comparison. Net I is sparse. The correlation between each pair of stations is small. Hence the optimal weights are approximately the same as the optimal weights, and the optimal weighting results are close to the uniform weighting results as shown in the first column of the table. Net II and AK Net are dense enough to show the effectiveness of the optimal weights for reducing the sampling error. The effect of the optimal weighting is more drastic for a more dense network, Net IV, which can sample the first ten modes with almost no error if the measured data are processed by the optimal weighting scheme.

Figure 4 shows the dependence of the percentage sampling errors and the signal-noise ratios on the spherical harmonic mode number up to the component as high as T_{66}. Figure 4(a), (b), (c), and (d) are for Net I, Net II, AK Net and Net IV, respectively. The mode numbers are rearranged in the way that: (00) = 1, (10) = 2, (11) = 3, (20) = 4, (21) = 5, (22) = 6, (30) = 7, etc. In this figure, we show the results up to (66) = 28. Only the modes with a positive rank are considered because the MSE formula (24) is symmetric with respect to m. Both Figure 4 and Table 1 seem to suggest that: (a) the percentage sampling error increases linearly with respect to the mode number arranged as above; and (b) the sampling error reduction versus the increment of the number of measurement stations is a highly nonlinear relationship.

Table 1. Percentage sampling error (V) and signal-to-noise ratio (Λ) in estimating the first ten spherical harmonic components using four different networks. Listed are two sets of experiments with optimal weighting scheme and uniform weighting scheme (in parenthesis), respectively.

	Net I N=24	Net II N=64	AK Net N=62	Net IV N=210
$V_{(00)}$	10 (10)	3.0 (15)	4.0 (11)	0.3 (13)
$\Lambda_{(00)}$	8.7 (8.7)	32 (5.9)	24 (8.1)	347 (6.6)
$V_{(10)}$	13 (15)	2.3 (36)	5.0 (23)	0.2 (35)
$\Lambda_{(10)}$	6.5 (5.9)	43 (1.8)	19 (3.4)	439 (1.9))
$V_{(11)}$	15 (15)	5.2 (9.3)	5.8 (10)	0.5 (7.0)
$\Lambda_{(11)}$	5.7 (5.5)	18 (9.7)	16 (8.7)	185 (13))
$V_{(20)}$	27 (27)	5.0 (64)	7.7 (39)	0.6 (63)
$\Lambda_{(20)}$	2.7 (2.7)	19 (0.6)	12 (1.5)	172 (0.6))
$V_{(21)}$	18 (24)	5.6 (7.1)	9.8 (18)	0.6 (3.4)
$\Lambda_{(21)}$	4.5 (3.2)	17 (13)	9.2 (4.5)	160 (29)
$V_{(22)}$	25 (30)	11 (14)	10 (17)	1.1 (8.8)
$\Lambda_{(22)}$	2.9 (2.4)	8.2 (6.3)	8.8 (5.0)	88 (10)
$V_{(30)}$	43 (45)	9.1 (79)	11 (53)	1.0 (79)
$\Lambda_{(30)}$	1.3 (1.2)	9.9 (0.3)	8.4 (0.9)	96 (0.3)
$V_{(31)}$	36 (42)	9.4 (20)	17 (37)	1.1 (14)
$\Lambda_{(31)}$	1.8 (1.4)	9.6 (4.0)	4.9 (1.7)	92 (6.1)
$V_{(32)}$	37 (39)	12 (13)	16 (24)	1.4 (4.8)
$\Lambda_{(32)}$	1.7 (1.6)	7.0 (6.8)	5.3 (3.1)	68 (20)
$V_{(33)}$	40 (55)	22 (22)	18 (29)	2.5 (10)
$\Lambda_{(33)}$	1.5 (0.8)	3.6 (3.5)	4.6 (2.4)	39 (8.8)

7 Conclusions

We have estimated the mean square errors (MSE) for sampling various orders of spherical harmonics of the surface temperature anomalies. The assumptions taken are as follows: (i) the statistics is homogeneous, (ii) the only low frequency limit is considered, and (iii) the spectra of the covariance field can be computed from a noise forced energy balance model. Both the analytic and numerical results indicate that: (a) the percentage sampling error increases with respect to the order of the spherical harmonic function; (b) the optimal weights are effective in reducing the sampling error and the optimal weighting scheme is strongly recommended for estimating the spherical harmonic components, and (c) there are sampling networks that result in zero sampling errors from the lower order spectra. With about 60 reasonably positioned stations for sampling the spherical harmonic components T_{00}, T_{10} and T_{11}, one can get the sampling error below 10% when the optimal weights are applied. An experiment with 210 stations leads to sampling error less than 10% for the spherical harmonic components from T_{00} up to T_{54}.

The major advantage in assuming the homogeneous statistics and an energy balance model with constant coefficients is that the mathematical formulation becomes simple while some important physical properties still remain, and hence some relevant physical properties become transparent. But, of course, the simple energy balance model leaves out lots of fine structures, such as the dynamical ENSO (El Niño Southern Oscillation) pattern. The spectra computed from the simple model certainly are much distorted from the real climate particularly for high order spherical harmonics. Notwithstanding this point, the methodology we provide here is still valid for exploring the sampling error for both homogeneous and inhomogeneous fields as long as EOFs and their corresponding variances can be obtained from data or a model. Therefore, the computation of the spectrum itself stands out as a very significant problem for detection and prediction (Kim and North, 1993).

ACKNOWLEDGEMENTS

The authors gratefully acknowledge support from a grant from the US Department of Energy "Quantitative Links" program. Shen thanks Environment Canada for a subvention grant by Atmospheric Environment Service.

REFERENCES

Arfken, G. (1985). *Mathematical Methods for Physics.* 3rd ed., San Diego: Academic Press.

Folland, C. K., T. R. Karl, N. Nicholis, B. S. Nyenzi, D. E. Parker, and K. Ya. Vinnikov (1992).'Observed climate variability and change'. In *Climate change, the IPCC Scientific Assessment*, eds. J. T. Houghton, B. A. Callander, and S. K. Varney. London: Cambridge University Press, 135–170.

Hansen, J., and S. Lebedeff (1987). 'Global trends of measured surface air temperature'. *J. Geophys. Res.* **92**, 13345–13372.

Hardin, J. W., G. R. North, and S. S. Shen (1992). 'Minimum error estimates of global mean temperature through optimal arrangement of gauges'. *Environmetrics* **3**, 15–27.

Kim, K.-Y., and G. R. North (1991). 'Surface temperature fluctuations in a stochastic climate model'. *J. Geophys. Res.* **96**, 18573–18580.

——, and ——(1993). 'EOF analysis of surface temperature field in a stochastic climate model'. *J. Climate* **6**, 1681–1690.

North, G. R., S. S. Shen, and J. W. Hardin (1992). 'Estimation of the global mean temperature with point gauges'. *Environmetrics* **3**, 1–14.

Shen, S. S., G. R. North, and K.-Y. Kim (1994). 'Spectral approach to optimal estimation of the global average temperature'. *J. Climate* **7**, 1999–2007.

Trenberth, K. E., and J. G. Olson (1992). 'Representativeness of a 63-station network for depicting climate changes'. In *Greenhouse-Gas-Induced Climatic Change: A Critical Appraisal of Simulations and Observations*, eds. M. E. Schlesinger, New York: Elsevier, 249–259.

Figure Captions

Figure 1. The relationship between the length scale λ_0 and the zeroth order Fourier-Legendre coefficient ρ_0 of the correlation function $\rho(x)$.

Figure 2. The percentage sampling error of randomly distributed stations $RV_{(lm)}^{[N]}$ where the length scale $\lambda_0 = 0.3141$ [in units of radius of the Earth]. The numerical results are based upon the formula (61). The four curves correspond to the mode $l = 0$, 1, 2 and 3, respectively (in an ascending order).

Figure 3. The signal-noise ratio resulted from sampling with randomly distributed stations $R\Lambda_{(lm)}^{[N]}$ where the length scale is the same as that of Figure 2. The numerical results are based upon the formula (60). The four lines correspond to the mode $l = 0$, 1, 2 and 3, respectively (in an descending order).

Figure 4. The dependence of the percentage sampling error and the signal-noise ratio on the spherical harmonic mode number for Net II. Here, the optimal weights are used and the mode numbers are rearranged in the way that: $(00) = 1$, $(10) = 2$, $(11) = 3$, $(20) = 4$, $(21) = 5$, $(22) = 6$, $(30) = 7$, $\cdots$, $(66) = 28$. Panel (a) is for Net I, (b) for Net II, (c) for the AK Net, and (d) for the dense network, Net IV, of 210 stations.

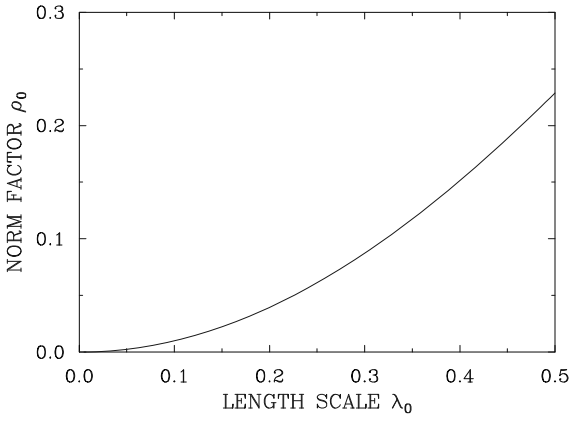

Figure 1. The relationship between the length scale λ_0 and the zeroth order Fourier-Legendre coefficient ρ_0 of the correlation function $\rho(x)$.

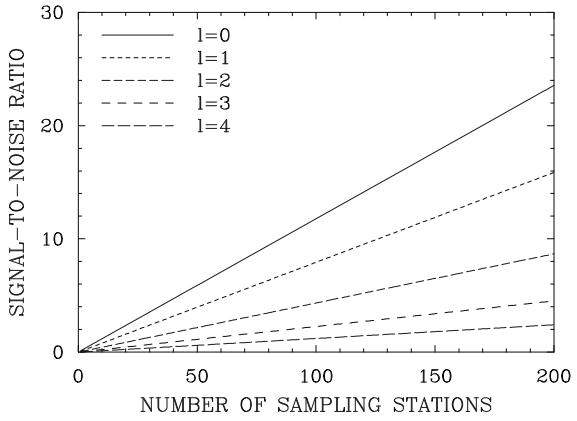

Figure 2. The percentage sampling error of randomly distributed stations $RV_{(lm)}^{[N]}$ where the length scale $\lambda_0 = 0.3141$ [in units of radius of the Earth]. The numerical results are based upon the formula (61). The four curves correspond to the mode $l = 0$, 1, 2 and 3, respectively (in an ascending order).

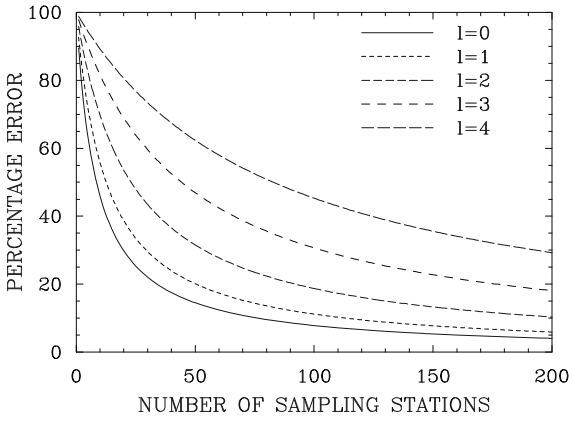

Figure 3. The signal-noise ratio resulted from sampling with randomly distributed stations $R\Lambda_{(lm)}^{[N]}$ where the length scale is the same as that of Figure 2. The numerical results are based upon the formula (60). The four lines correspond to the mode $l = 0$, 1, 2 and 3, respectively (in an desending order).

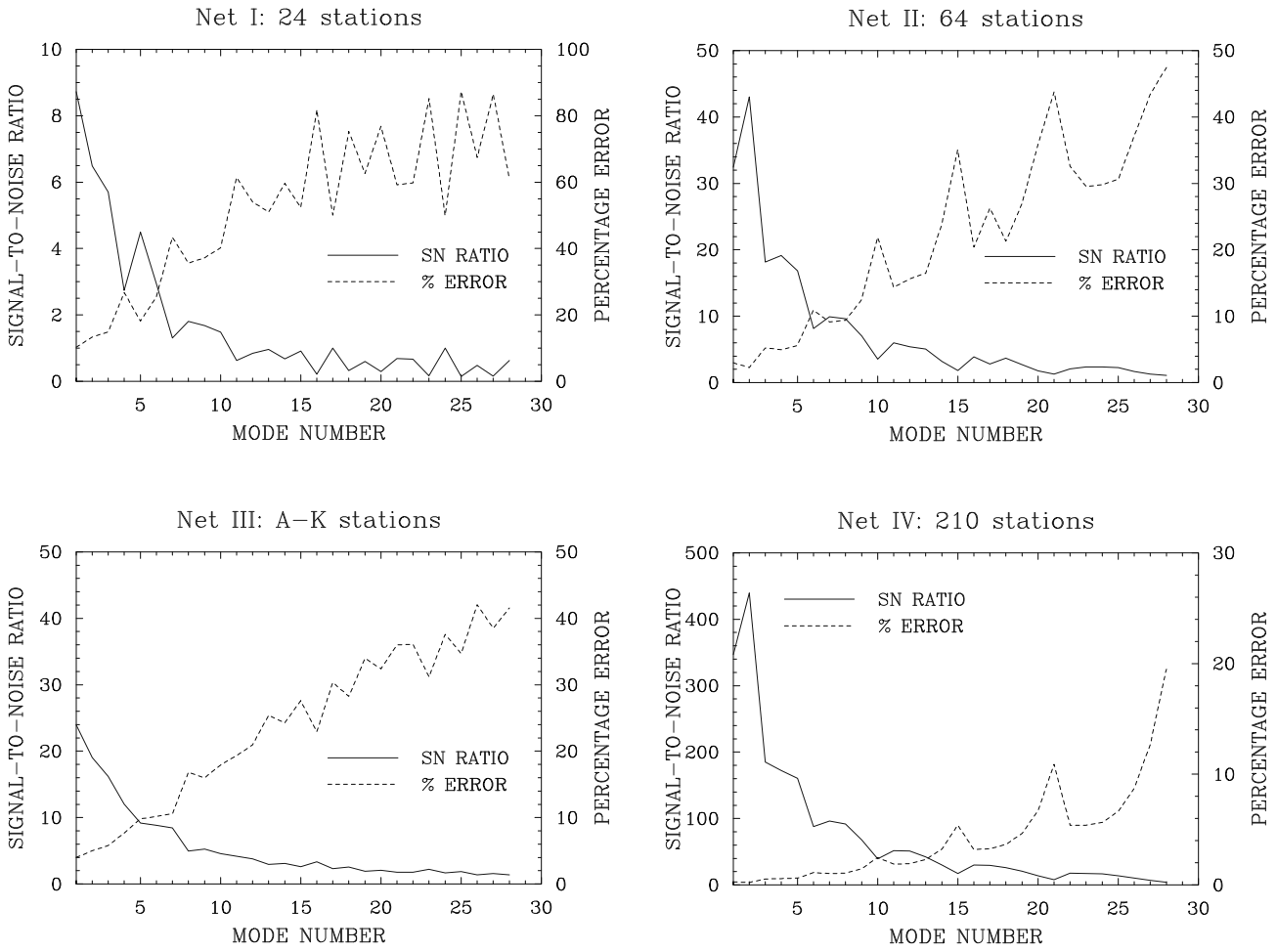

Figure 4. The dependence of the percentage sampling error and the signal-noise ratio on the spherical harmonic mode number for Net II. Here, the optimal weights are used and the mode numbers are rearranged in the way that: $(00) = 1$, $(10) = 2$, $(11) = 3$, $(20) = 4$, $(21) = 5$, $(22) = 6$, $(30) = 7$, $\cdots$, $(66) = 28$. Panel (a) is for Net I, (b) for Net II, (c) for the AK Net, and (d) for the dense network, Net IV, of 210 stations.